

## Numerical Model of a 3D-Printed Titanium Structure For Use in Implant Dentistry

ŘEHOUNEK Luboš<sup>1, a</sup>, JÍRA Aleš<sup>1, b</sup> and DENK František<sup>1, c</sup>

<sup>1</sup> Department of Mechanics, Czech Technical University in Prague, Thákurova 7; 166 29, Prague; Czech Republic

<sup>a</sup> lubos.rehounek@fsv.cvut.cz, <sup>b</sup> jira@fsv.cvut.cz, <sup>c</sup> frantisek.denk@fsv.cvut.cz

**Keywords:** Numerical Model, 3D Printing, Titanium, Biomechanics, Trabecular.

**Abstract.** The aim of this work is to describe the mechanical behavior of the novel trabecular structure. It is a porous structure that comprises of beams of equal length embedded into a 3D matrix. 3D printing was used to create test specimens. To determine the values of Young's modulus  $E$  and reduced modulus  $E_r$ , we performed nanoindentation and tensile and compression tests. The tensile test was then used as a baseline for the development of a numerical model. The next effort will be to apply the model onto a real implant that was invented and patented in Czech Republic.

### Introduction

The trabecular structure has only recently been recognized as a viable option for dental restorations and other prosthetics. There are no known documented material tests yet, and since the parameters of every structure can be different, the outcomes may significantly vary. The stress-strain diagrams of this specific structure were provided by uniaxial tests. These tests were carried out on specifically designed implant specimens shown in Fig.1. Traditionally machined implants have a long history of success [1, 2], but they are still prone to failure in the early stages of the bonding process, because the surface properties play an important role in osseointegration [3]. The trabecular structure can potentially have many benefits, such as increased osseointegration, reduced stress-shielding and lower modulus [4]. This reduction is a significant benefit because it provides a smoother transition region in between the faces of the dental materials. The trabecular shell of an implant (Fig. 7) also provides an environment for bone ingrowth, as opposed to conventional implants, which only allow for bone ongrowth. The specimens were 3D-printed using the M2 Cusing Concept Laser machine and a specialized Rematitan Cl metal powder in cooperation with ProSpon spol. s. r. o.



a) compression test specimen



b) tensile test specimen

Fig. 1: Trabecular structure specimens for global mechanical tests and nanoindentation.

## Trabecular Structure

Since the structure is porous, its geometry allows for bone ingrowth and creates a scaffold for the bone cells to grow into [5, 6]. With conventional implants, bone cells are only able to grow onto the surface of the implant. With the trabecular structure, the cells can grow inside and create an interconnected material comprising of both bone and metal bonded together (Fig. 2).

**Osseointegration.** The trabecular structure can potentially provide better osseointegration because its morphology resembles a material with high surface roughness (trabecular portion, Fig. 2 left). This assumption is, however, still to be proven as there is not enough evidence and history to support this claim. Surface roughness has been proven to play an important role in the bonding process [7]. The greater the surface area of the implant, the greater the interlocking between the implant surface and bone.

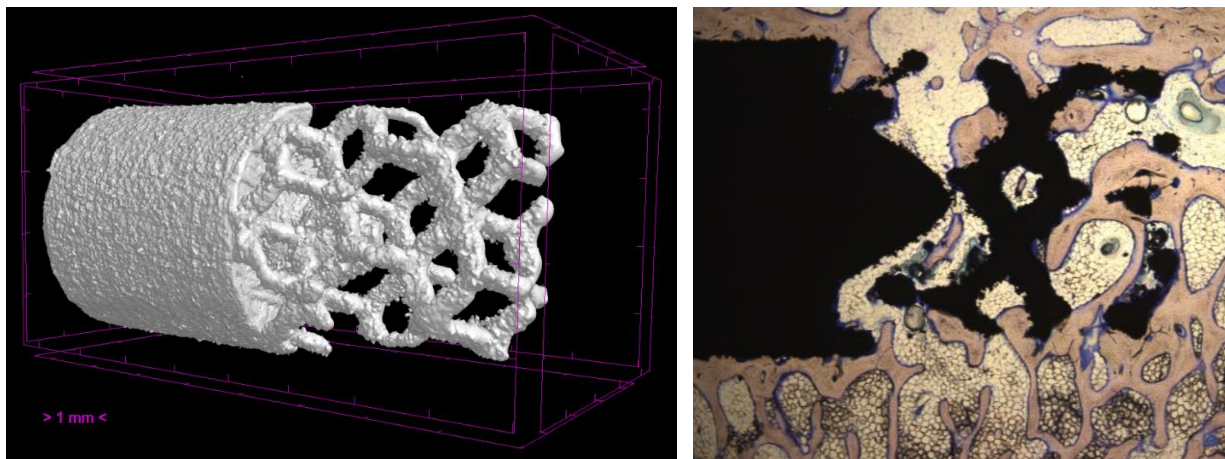


Fig. 2: Scaled micro-CT scan of the implant specimen with a trabecular end portion (left) and a micrograph of a longitudinal section of an extracted implant (right). White and light yellow color represents the beams of newly formed bone, orange represents fibrous tissue and black color represents the trabecular implant. These figures were obtained from in-vivo tests of the trabecular implants.

**Young's Modulus.** It is very important to distinguish between the values of Young's modulus and reduced modulus. The reduced modulus of the material remains unchanged, but the Young's modulus is reduced as the cross-section area of the implant is also reduced (Fig. 3). One of the causes of implant failure during the early stages of osseointegration is its loosening. This reduction eliminates the concentration of stresses in the intraosseous implant stem and is beneficial to the healing process.

**Stress-Shielding.** Stress-shielding is an unwanted factor that represents uneven distribution of stress between the implant, peri-implant area and bone [8]. The values of Young's modulus of human bone are significantly lower (approximately 20-30 GPa [9]) than those of the implant (90-110 GPa for conventional titanium implants [4]), the bone is left without sufficient stimulus and the stresses are transferred into the implant.

When the bone material is not subjected to sufficient loads, it becomes overly porous and is no longer able to hold the implant in position, making it eventually slip out, resulting in

failure of the implant. This is true due to the fact that bone is always adapting to the conditions it is placed under. This process is described by the Wolff's law [10].

### Mechanical Tests

**Nanoindentation.** In order to determine the values of properties on the micro level, we performed nanoindentation tests considering reduced modulus of elasticity, hardness and contact depth. The nanoindentation tests were performed using the Oliver & Pharr method and their main purpose was to compare the conventional Ti-6Al-4V machined material to our 3D-printed specimens. The micromechanical analysis was performed using the CSM Instruments nanoindenter in the mode of directed force and repeated loading. The load program was set with consideration of eliminating surface tension and shear stiffness in the atomic material structure. The values of reduced modulus  $E_r$  were in the range of 118-131 GPa.

**Uniaxial Tests.** For the purpose of global mechanical tests, we used the 3D Dode-Thick [MSG] structures with dimensions of 14×14×14 mm (a cube for the compression test) and a 14×14×42 mm (a block for the tensile test). A total of 9 specimens were tested beyond the point of failure on the MTS Alliance RT-30 machine. The results of the tests are shown in Tab. 1.

Tab. 1: Values of Young's modulus obtained by global mechanical analysis.

Young's modulus E [MPa]										
Specimen	1	2	3	4	5	6	7	8	9	Mean
Tens. test	964.7	975.9	982.2	-	-	-	-	-	-	<b>974.3</b>
Comp. test	-	-	-	1114.2	1080.6	947.2	818.8	999.6	803.8	<b>960.7</b>

By incorporating the trabecular structure, we were able to reduce the modulus more than 100 times as compared to traditionally machined implants [4]. This reduction is connected with the reduction of the cross-section area (Fig. 3). This outcome is purely experimental as the structure does not have any documented material tests and its morphology is individual. However, we believe that the values of modulus do not necessarily need to exactly match human bone as more aspects come into consideration. These aspects are such as magnitude of pores, their geometry or character of bone ingrowth in relation to the geometry of the structure.



a) homogeneous (full) cross-section of an implant test specimen



b) trabecular cross-section of an implant test specimen

Fig. 3: Micrographs of full and trabecular cross-sections of an implant test specimen. Note the difference between the cross-section area, which is reduced approximately by 90%.

### Numerical Model

**Geometry.** The geometry of the model was created in order to minimize the computational requirements. Since the original geometry contained too many beams and its use would be complicated, we decided to create a new geometry that would require fewer elements. Comparison of the two geometries is shown in Fig. 4 and Fig. 5. This new geometry shown in Fig. 5 used only three basic structure elements per an edge of the imaginary circumscribing cube. This reduction has proven to be beneficial as the computation times decreased.

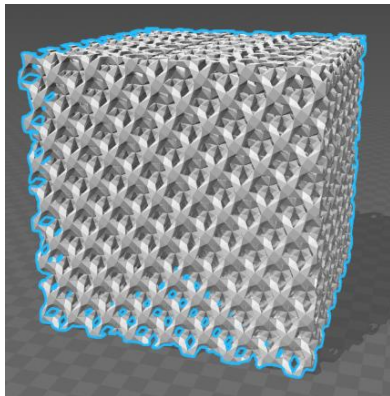


Fig. 4.: The former STL file used to create the test specimens.

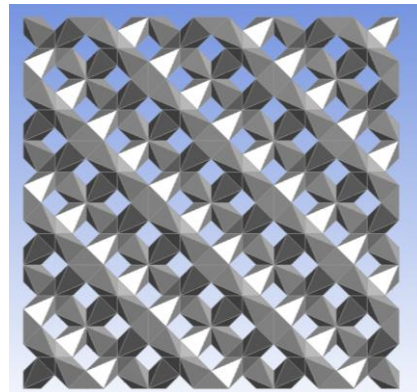


Fig. 5: The new 3D geometry created in Ansys Workbench Design Modeler.

**Curve-fitting.** There is only one time-dependent load (the displacement recorded by the machine), so the analysis can be performed in one computation step. We were trying to curve-fit the stress-strain diagram of the tensile test of specimen number 3 (Fig. 6 black). The convergence of the solution was attained by the Newton-Raphson method. We used the Ti-6Al-4V material model with a bilinear stress-strain diagram with isotropic hardening.

In order to create the virtual material's properties, we experimentally manipulated the values of mechanical properties in the model. The final values which have been fine-tuned during the curve-fitting process were saved and recorded for further development of the model. The final curve is shown in Fig. 6.

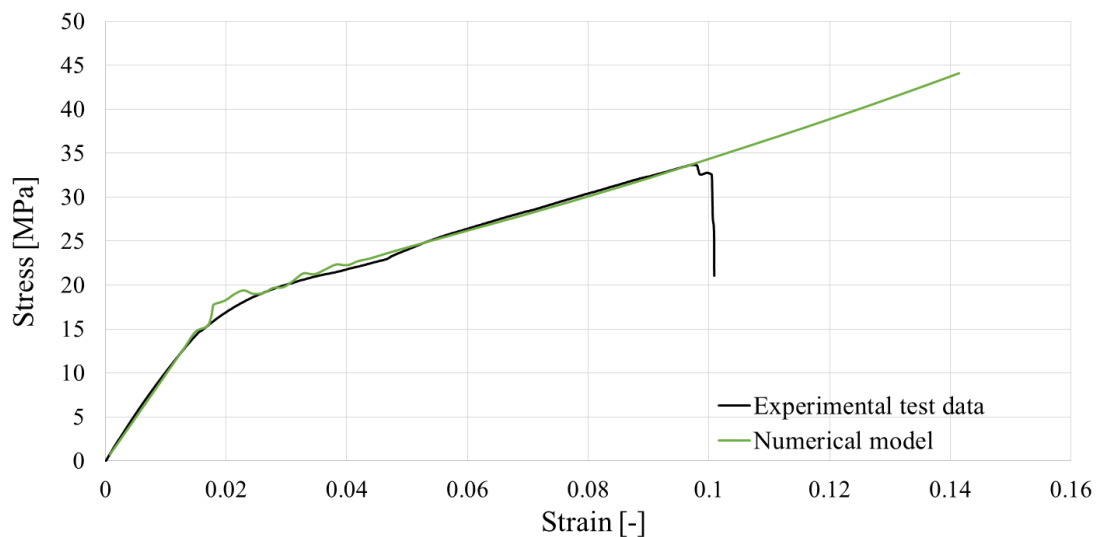


Fig. 61: The final achieved curve of the numerical model (green) compared to the tensile test stress-strain diagram of specimen number 3 (black). The model did not achieve failure beyond the range of ultimate strength, which is an acknowledged fact and will be addressed in our future efforts.

**Future Prospects of the Model.** The first feature of the model that needs to be addressed is the unattained failure. This is due to the fact that the solver cannot, by default, provide an accurate solution beyond the range of ultimate strength for this material model. We expect that we will be able to solve this shortcoming by adding additional algorithms to the solver.

The next major step is to apply this numerical model on a real implant. This implant has been invented and patented in Czech Republic and is shown in Fig. 7 (middle). On the basis of the patent application PV 2014-795, the patent n.306457 has been granted for the „four clover“ implant variant by authors F. Denk Jr., A. Jira and F. Denk Sr [11]. The methodology will probably comprise of applying the numerically obtained properties of the virtual material onto a homogeneous structure that will substitute the trabecular outer shell of the implant (Fig. 7 right).

## Conclusions

The main benefits that the trabecular structure can introduce are bone ingrowth, reduced modulus and reduction of stress-shielding. We have been able to successfully determine the values of the trabecular’s structure modulus (Tab. 1), which is over a 100 times lower than the modulus of conventionally machined homogeneous implants [4], but other assumptions are still to be proven true with time and more experiments. This reduction is beneficial as the mechanical properties of the implant are more similar to human bone. The curve-fitting process was completed successfully with the exception of attaining failure beyond the range of ultimate strength, which is going to be addressed in our future work. The trabecular structure, unlike conventional homogeneous structures, allows for both bone ongrowth and ingrowth.

With the curve-fitted material properties available, we will be able to determine the mechanical behavior of an implant comprising of a homogeneous stem and a trabecular outer shell (Fig. 7). This conjunction will be the final purpose of the model. The STL files needed to create the model and merge the two materials together are already available to us (Fig. 7 left). However, since the full analysis of the trabecular structure would be very demanding in computation times, it is expected that its mechanical properties will be applied onto a homogeneous cross-section (Fig. 7. right).

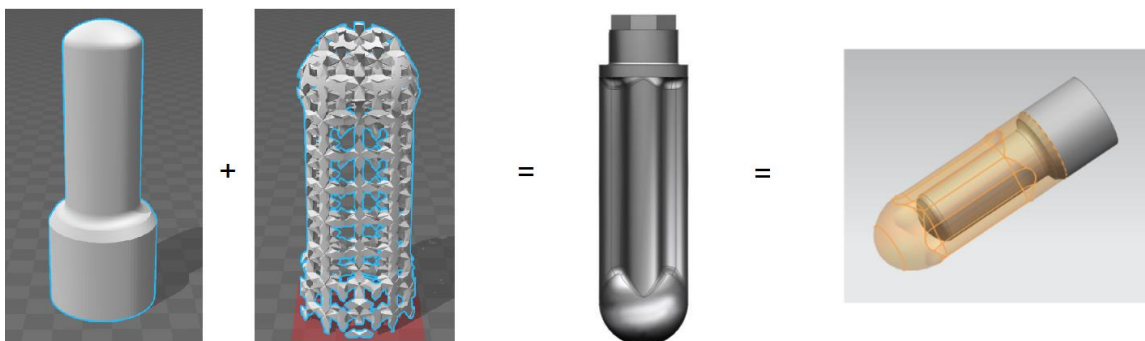


Fig. 7: The “four leaf clover” implant variant, comprising of a cylindrical body and four rounded grooves encompassed in a hemisphere (in the middle) and the two potential approaches towards modelling the structure. Two STL files for direct characterization (left) and a model using the homogenized structure (right).

## **Acknowledgement**

The financial support by the Faculty of Civil Engineering, Czech Technical University in Prague (SGS project No. SGS17/168/OHK1/3T/11) is gratefully acknowledged.

## **References**

- [1] T. Hasegawa et al., Survival of Brånemark System Mk III implants and analysis of risk factors associated with implant failure, *Int. J. Oral Maxillofac. Surg.*, 46 (2016) 267–273.
- [2] F. De Angelis, P. Papi, F. Mencio, D. Rosella, S. Di Carlo, and G. Pompa, Implant survival and success rates in patients with risk factors: results from a long-term retrospective study with a 10 to 18 years follow-up, *Eur. Rev. Med. Pharmacol. Sci.*, 21 (2017) 433–437.
- [3] L. Le Guéhennec, A. Soueidan, P. Layrolle, and Y. Amouriq, Surface treatments of titanium dental implants for rapid osseointegration, *Dent. Mater.*, 23 (2007) 844–854.
- [4] M. Niinomi, Mechanical properties of biomedical titanium alloys, *Mater. Sci. Eng. A*, 243 (1998) 231–236.
- [5] F. E. Wiria, J. Y. M. Shyan, P. N. Lim, F. G. C. Wen, J. F. Yeo, and T. Cao, Printing of Titanium implant prototype, *Mater. Des.*, 31 (2010) 101–105.
- [6] A. El-Hajje et al., Physical and mechanical characterisation of 3D-printed porous titanium for biomedical applications, *J. Mater. Sci. Mater. Med.*, 25 (2014) 2471–2480.
- [7] K. Gotfredsen, T. Berglundh, and J. Lindhe, Anchorage of titanium implants with different surface characteristics: an experimental study in rabbits, *Clin. Implant Dent. Relat. Res.*, 2 (2000) 120–128.
- [8] M. I. Z. Ridzwan, S. Shuib, A. Y. Hassan, A. A. Shokri, and M. N. Mohammad Ibrahim, Problem of stress shielding and improvement to the hip implant designs: A review, *Journal of Medical Sciences*, 7 (2007) 460–467.
- [9] J. Y. Rho, R. B. Ashman, and C. H. Turner, Young's modulus of trabecular and cortical bone material: Ultrasonic and microtensile measurements, *J. Biomech.*, 26 (1993) 111–119.
- [10] S. C. Cowin and D. H. Hegedus, Bone remodeling II: theory of adaptive elasticity, *J. Elast.*, 6 (1976) 313–326.
- [11] F. Denk Sr., F. Denk Jr. and A. Jíra, CZ Patent 306,457. (2017)